

Energy Consumption in RES-aware 5G Networks

Adam Samorzewski

Poznan University of Technology
Poznan, Poland

adam.samorzewski@doctorate.put.poznan.pl

Margot Deruyck

Ghent University – IMEC
Ghent, Belgium

margot.deruyck@ugent.be

Adrian Kliks

Poznan University of Technology
Poznan, Poland

adrian.kliks@put.poznan.pl

Abstract—In this work, the impact of using Renewable Energy Source (RES) generators in next-generation (5G) cellular systems on total power consumption (PC) has been investigated. The paper highlights the gain related to the use of photovoltaic (PV) panels and wind turbines (WTs) in the form of two factors – the average extension of battery lifetime (AEBL) powering a single network cell and the average reduction in energy consumption (AREC) within the whole network. The examination has been conducted for four different seasons of the year and various configurations of available power sources. The provided system scenario was based on real data on weather conditions, building placement, and implemented mobile networks for the city of Poznan in Poland. Used RES generators were designed in accordance with the specifications of real devices.¹

Index Terms—5G, energy models, green networks, power consumption, Renewable Energy Sources, wireless systems

I. INTRODUCTION

Today, the ICT sector is still responsible for huge emissions, which are systematically underestimated and could actually be as high as 2.1 to 3.9% of the global GHG (Green House Gas) emissions [1]. Networks – both wired and wireless – contribute about 25% to this value. Within the wireless network, the base station (BS) is the largest consumer. Even though the hardware is becoming more energy-efficient, a 5G BS consumes about 4 times more energy compared to a 4G one [2]. A 5G BS does provide a 16 times higher throughput, but the 5G network will be more dense, increasing the network’s energy consumption by 150 to 170% by 2026 [2]. One way to deal with the impact of this rise in energy consumption is the use of renewable energy sources (RESs) such as e.g., solar, wind, water, or geothermal energy. By using RESs, we can not only reduce emissions but also protect our fossil fuels from future depletion. Unfortunately, due to the fluctuating provisioning of some RESs (because of varying weather conditions), their use in wireless networks has not been widely investigated yet. In this paper, we build upon the work of [3] and [4] by investigating

the use of solar and wind energy for a large-scale 5G network in the city of Poznan, Poland. The novelty of the study lies in: suitable power consumption models for 5G and its features like massive MIMO (Multiple Input Multiple Output) are now included for various frequencies (800, 2100, 3500 MHz); weather prediction models based on real historical data for the city of Poznan, Poland; and (dis)charging and transportation losses are considered for four scenarios accounting for solar or wind energy or both.

II. METHODOLOGY

A. Network Design

For this study, the network planner discussed in [4] is further extended. This planner called GRAND (Green Radio Access Network Design) is a deployment tool that designs and optimizes wireless outdoor access networks toward power consumption and/or human exposure by selecting the optimal base station locations and settings based on the instantaneous bit rate request of the users active in the environment. The tool takes various inputs such as a shape file describing the 3D environment for which the network will be optimized, a list of possible base station locations, and a list of active users, their locations, and their bit rate requests. In the first step, the tool makes a list of potential base stations to connect each user with (based on the user’s bit rate request and the maximum allowable path loss). Once this graph of base station-user associations is made, a MIP (Mixed Integer Programming) solver is applied to find the optimal solution. To this end, an objective function is defined based on the envisioned optimization of power consumption, human exposure, or both.

B. Renewable Energy Sources

In order to reduce the use of energy from the conventional electrical grid, it was considered to power the wireless network with PV panels and wind turbines. Furthermore, to reduce the loss of harvested resources, each base station has been equipped with a battery system to store the excess energy. The processes of energy generation were modeled within the GRAND tool in accordance with the works contained in [5]–[11] and widely described in Section IV. In addition, the parameters for both types of RES generators as well as for the battery were implemented with respect to the specifications of real devices, which can be found in [12]–[14].

¹Copyright © 2023 IEEE. Personal use is permitted. For any other purposes, permission must be obtained from the IEEE by emailing pubpermissions@ieee.org. This is the author’s version of an article that has been published in the proceedings of the 2023 IEEE Global Communications Conference (GLOBECOM) by the IEEE. Changes were made to this version by the publisher before publication, the final version of the record is available at: <https://dx.doi.org/10.1109/GLOBECOM54140.2023.10437451>. To cite the paper use: A. Samorzewski, M. Deruyck and A. Kliks, “Energy Consumption in RES-Aware 5G Networks,” *GLOBECOM 2023 – 2023 IEEE Global Communications Conference*, Kuala Lumpur, Malaysia, 2023, pp. 1024–1029, doi: 10.1109/GLOBECOM54140.2023.10437451 or visit <https://ieeexplore.ieee.org/document/10437451>.

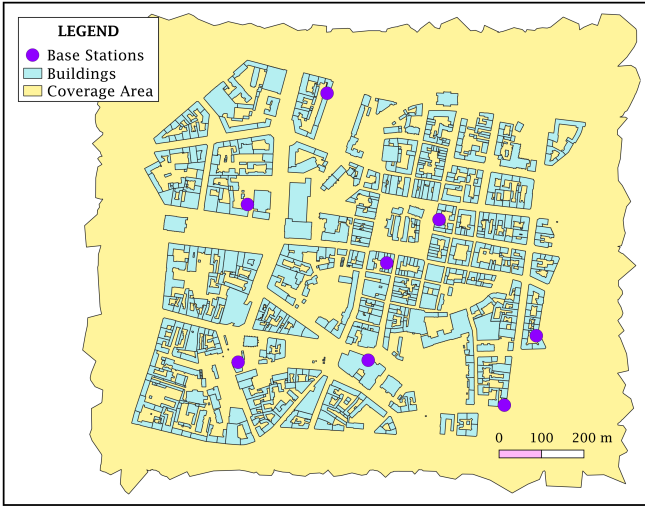


Fig. 1. Map of the examined area within the city of Poznan.

III. SCENARIO

In the examined scenario (illustrated in Fig. 1), the mobile network within the old market area of Poznan (Poland) was considered. In the very beginning, we assumed 8 locations within the city, at which 5G base stations are placed (designed on the basis of plans of the city of Poznan [15] and data of one Polish mobile operator given in [16]). Each BS is mounted on one of the buildings and has 3 cells using different frequency bands – 800, 2100, and 3500 MHz. In addition, cells configured in the third band were deployed to use Massive MIMO technology, which affects power consumption and signal propagation gain. For each hardware set of each cell type, there is a separate container (outside room) with air conditioners next to the BS tower. All the data about the placement of buildings and access nodes in the area as well as about the weather conditions were taken from the databases of historical records contained in [15]–[17]. Between buildings, there are 300 outdoor users with dedicated equipment (UE), whose standings and throughput demands are fixed. All the locations of users are selected randomly within the simulator for each single run. Firstly, all the network cells are set to broadcast the radio signal with the maximum power. After distributing users within the examined area, the GRAND tool starts assigning them among the cells while optimizing cells’ transmit powers and ensuring users’ bit rate demands, simultaneously. Then, users begin exchanging data with the network continuously generating fixed traffic throughout the whole time of a simulation run. Within a single run, the calculations have been performed for four different dates (each from a different season of the year) to investigate the impact of time of the day and year on the energy harvesting characteristics of both RES types.

IV. ENERGY MODELS

In this section, the mathematical formulas for modeling processes of energy consumption and production (prosumption)

by the designed system have been presented.

A. MIMO Base Station

The model used to estimate the power consumption by 5G base stations has been formulated in accordance with the work contained in [5]. In this contribution, from the perspective of energy cycle modeling, all the cells have been considered to be Massive MIMO (whether they are or not) using a different number of active antenna elements (AAEs), i.e., 5G 800 and 5G 2100 – 1 AAE, 5G 3500 – 64 AAEs. The mathematical formula that evaluates the total power consumption (P_{MIMO}) by a single cell in the current time step t is as below:

$$P_{\text{MIMO}}(t) = P_{\text{CP}}(t) + P_{\text{PA}}(t) + \frac{P_{\text{cool}}(t)}{1 - \sigma_{\text{cool}}} + P_{\text{AUX}}(t), \quad (1)$$

where $P_{\text{PA}}(t) = \frac{P_{\text{TX}}(t)}{\mu_{\text{PA}}}$ is the power consumed by the power amplifier. The parameters of P_{TX} and μ_{PA} are the transmit power and efficiency of the amplifier, respectively. In turn, σ_{cool} is the cooling loss factor. Next, the P_{CP} , P_{cool} , and P_{AUX} are the powers spent by the transceiver, cooling, and auxiliary hardware components. The latter refers to additional equipment not related to providing the radio connection (e.g., lighting). The former was expressed as follows:

$$P_{\text{CP}}(t) = P_{\text{FIX}} + P_{\text{TC}}(t) + P_{\text{CE}}(t) + P_{\text{CD}}(t) + P_{\text{BH}}(t) + P_{\text{SP}}(t), \quad (2)$$

where P_{FIX} is the fixed power consumed by a cell node. The parameter of $P_{\text{TC}}(t) = M_{\text{BS}}(t) P_{\text{CC}}$ is the power utilized by the transceiver chains in the time step t , where P_{CC} is the power that is required to run the circuit components (e.g. filters, I/Q mixers, etc.), and M_{BS} is the number of presently active antenna elements of the cell. Next, $P_{\text{CE}}(t) = \frac{3B_w}{\tau_c \cdot \eta_{\text{BS}}} K_{\text{UE}}(t) (M_{\text{BS}}(t) \tau_p(t) + M_{\text{BS}}^2(t))$ is the power needed by the channel estimators, which work according to the minimum mean-squared error (MMSE) scheme [5]. The parameters of B_w and η_{BS} are the channel bandwidth and computational efficiency, respectively. In addition, $\tau_p(t) = \text{RF} \cdot K_{\text{UE}}(t)$ is the number of samples allocated for pilots per coherence block in a specific time step t , where RF is the pilot reuse factor and K_{UE} is the current number of served users. In turn, $\tau_c = B_c \cdot t_c$ is the number of samples per coherence block, where B_c and t_c are the coherence bandwidth and time, respectively. Furthermore, $P_{\text{CD}}(t) = P_{\text{COD}} \cdot \text{TR}_{\text{DL}}(t) + P_{\text{DEC}} \cdot \text{TR}_{\text{UL}}(t)$ is the total power consumed by a single cell of the BS for encoding (P_{COD}) and decoding (P_{DEC}) the information transferred through uplink, in short UL, (TR_{UL}) and downlink, in short DL, (TR_{DL}) connections in a particular time step t . The power model takes into account also the load-aware part of the consumption referring to the backhaul links – $P_{\text{BH}}(t) = P_{\text{BT}}(\text{TR}_{\text{UL}}(t) + \text{TR}_{\text{DL}}(t))$, where P_{BT} is the backhaul traffic power. Finally, the power required by the network cell for operations related to signal processing (e.g., UL reception

and DL transmission, computation of the combining/precoding vectors) compliant with the MMSE scheme (P_{SP}) is as below:

$$P_{SP}(t) = \frac{3B_w}{\tau_c \cdot \eta_{BS}} \left[M_{BS}(t) K_{UE}(t) (\tau_u(t) + \tau_d(t)) \right. \\ \left. + \frac{(3M_{BS}(t)^2 + M_{BS}(t)) K_{UE}(t)}{2} + \frac{M_{BS}(t)^3}{3} + 2M_{BS}(t) \right. \\ \left. + M_{BS}(t) \tau_p(t) (\tau_p(t) - K_{UE}(t)) + M_{BS}(t) K_{UE}(t) \right], \quad (3)$$

where $\tau_d(t)$ is the number of DL data samples per coherence block in the time step t .

The component P_{cool} in Eq. (1) represents the power that is necessary to keep the adequate temperature (T_s) inside the server rooms of the BS. The mathematical formula describing the power utilization for hardware cooling has been attached in Eq. (4), where σ_{CP} and $T_a(t, h_{BU})$ are the circuit heat transfer coefficient of the hardware placed inside the server room and the temperature of its outside ambient in the time step t , respectively. The parameter of h_{BU} denotes the ground-relative altitude of the building, on which a particular BS (as well as its server rooms and PV panels) is placed. Next, A_s and σ_s are the surface area and heat transfer coefficient of a specific server room storing the equipment of the cell. The former is equal to $A_s = 2a_s b_s + 2a_s h_s + 2b_s h_s$, where a_s , b_s , and h_s are the dimensions of the server room (container).

B. PV Panel

There is a need to model the energy harvesting process performed by PV panels supplying each cell of each BS tower. The output power of the set of PV arrays (P_{PV}) in a certain time step t can be denoted as [7]:

$$P_{PV}(t) = N_{PV} P_{R,PV} f_{PV} \cdot \frac{\bar{G}_T(t)}{\bar{G}_{T,STC}} \left[1 + \alpha_P (T_c(t) - T_{c,STC}) \right], \quad (5)$$

where N_{PV} , $P_{R,PV}$, and f_{PV} are the total number of PV panels allocated per network cell, and the rated power and derating factor of a single one. In addition, the first one is the multiplication of the numbers of PV panels connected in series ($N_{PV,s}$) and parallel ($N_{PV,p}$). Next, \bar{G}_T and T_c are the parameters that denote the solar radiation incident on the PV array and its temperature. Thus, $\bar{G}_{T,STC}$ and $T_{c,STC}$ define the values of the same parameters but for standard test conditions (STC). Finally, α_P is the temperature coefficient of power dependent on the type of used PV panels. Besides, to assess the temperature of the PV cell (T_c), the formula was used [7]:

$$T_c(t) = \frac{T_a(t, h_{PV})}{1 + (T_{c,NOCT} - T_{a,NOCT}) \left(\frac{\bar{G}_T(t)}{\bar{G}_{T,NOCT}} \right) \left(\frac{\alpha_P \mu_{mp,STC}}{\tau \alpha} \right)} \\ + \frac{(T_{c,NOCT} - T_{a,NOCT}) \left(\frac{\bar{G}_T(t)}{\bar{G}_{T,NOCT}} \right) \left[1 - \frac{\mu_{mp,STC} (1 - \alpha_P T_{c,STC})}{\tau \alpha} \right]}{1 + (T_{c,NOCT} - T_{a,NOCT}) \left(\frac{\bar{G}_T(t)}{\bar{G}_{T,NOCT}} \right) \left(\frac{\alpha_P \mu_{mp,STC}}{\tau \alpha} \right)}, \quad (6)$$

where $T_{c,NOCT}$, $T_{a,NOCT}$, and $\bar{G}_{T,NOCT}$ are the nominal operating cell temperature (NOCT) of the PV panel, and the ambient temperature and solar radiation at which the NOCT is defined, respectively. Next, τ , α , and $\mu_{mp,STC}$ are the solar transmittance of any cover over the PV array and its solar absorptance, and the maximum power point efficiency of the PV panel under STC. This efficiency is equal to $\mu_{mp,STC} = \frac{P_{R,PV}}{a_{PV} \cdot b_{PV} \cdot \bar{G}_{T,STC}}$, where a_{PV} and b_{PV} are the dimensions of a single PV module. In turn, the parameter of h_{PV} is the ground-relative altitude of the PV panels powering a specific cell.

C. Wind Turbine

Based on the contribution from [8], the output power in the time step t of a single wind turbine under standard test conditions ($P_{WT,STC}$) can be formulated as below:

$$P_{WT,STC}(t) = \begin{cases} F(v_w(t, h_{WT})), & \text{if } v_{in} \leq v_w(t, h_{WT}) \leq v_{out} \\ 0, & \text{otherwise} \end{cases}, \quad (7)$$

where h_{WT} , $v_w(t, h_{WT})$, and $F(v_w(t, h_{WT}))$ are the ground-relative altitude of the WT, wind speed at the altitude equal to h_{WT} at the current moment t , and the value of the power curve function (see [13]) of the WT for this wind speed, respectively. Conducting appropriate correction of $P_{WT,STC}$ parameter, it is possible to define the total power currently produced by the whole wind generators segment (P_{WT}) of a certain cell [7]:

$$P_{WT}(t) = N_{WT} \cdot P_{WT,STC}(t) \cdot \frac{\rho(t, h_{WT})}{\rho_{STC}}, \quad (8)$$

where ρ_{STC} and $\rho(t, h_{WT})$ are the air density at STC and the actual one at the level of h_{WT} in the current time step t . Finally, $N_{WT} = N_{WT,s} \cdot N_{WT,p}$ is the total number of used wind turbines, where $N_{WT,s}$ and $N_{WT,p}$ are the numbers of WTs connected to each other in series and parallel, respectively.

D. Battery System

Each cell has its own battery system to receive the energy from the RES generators. This system is also the first power source to satisfy a cell's electrical demand. Only when the accumulators cannot provide any energy, it is delivered from the power lines grid. Inspired by [9], we propose a new model of energy management within the battery system (E_{BATT}), which has been specified below:

$$E_{BATT}(t) = \begin{cases} E_{BATT}(t') + \Delta E_{BATT,1}(t), & \text{if } \Delta E(t) > 0 \\ E_{BATT}(t') + \Delta E_{BATT,2}(t), & \text{otherwise} \end{cases}, \quad (9)$$

where $E_{BATT}(t')$ is the energy handled by the battery system in the previous time step t' . Next, $\Delta E_{BATT,1}$ and $\Delta E_{BATT,2}$ are the energy amounts that have to be transferred from/to the battery system in the current time step t . Finally, ΔE is the energy balance, i.e., the difference between required energy and harvested one at the same moment. The parameters of $\Delta E_{BATT,1}$ and $\Delta E_{BATT,2}$ can be expressed by the formulas:

$$\Delta E_{BATT,1}(t) \\ = \max\left(\Delta E(t) \cdot \mu_{BATT}, E_{BATT,max} - E_{BATT}(t')\right), \quad (10)$$

$$P_{\text{cool}}(t) = \begin{cases} P_{\text{CP}}(t) \cdot \sigma_{\text{CP}} - A_s \cdot \sigma_s \cdot |T_s - T_a(t, h_{\text{BU}})|, & \text{if } T_s \geq T_a(t, h_{\text{BU}}) \text{ and } T_s - \frac{P_{\text{CP}}(t) \cdot \sigma_{\text{CP}}}{A_s \cdot \sigma_s} < T_a(t, h_{\text{BU}}) \\ P_{\text{CP}}(t) \cdot \sigma_{\text{CP}} + A_s \cdot \sigma_s \cdot |T_s - T_a(t, h_{\text{BU}})|, & \text{if } T_s < T_a(t, h_{\text{BU}}) \\ 0, & \text{otherwise} \end{cases} \quad (4)$$

$$\Delta E_{\text{BATT},2}(t) = \max \left(\frac{\Delta E(t)}{\mu_{\text{BATT}}}, -E_{\text{BATT}}(t') \right), \quad (11)$$

where μ_{BATT} and $E_{\text{BATT},\text{max}}$ are the efficiency of the used battery type and maximum energy the battery system is able to collect, respectively. The latter is equal to $E_{\text{BATT},\text{max}} = N_{\text{BATT}} E'_{\text{BATT},\text{max}}$, where $E'_{\text{BATT},\text{max}}$ is the maximum energy of a single battery, and $N_{\text{BATT}} = N_{\text{BATT},s} N_{\text{BATT},p}$ is the total number of accumulator units in a battery system. The parameters of $N_{\text{BATT},s}$ and $N_{\text{BATT},p}$ are the numbers of batteries linked to each other in serial and parallel order, respectively. To evaluate the current energy balance (ΔE), the formula below was engaged:

$$\Delta E(t) = \left(P_{\text{PV}}(t) + P_{\text{WT}}(t) - \frac{P_{\text{MIMO}}(t)}{1 - \sigma_{\text{DC}}} \right) (t - t'), \quad (12)$$

where σ_{DC} is the loss factor related to DC supplying the hardware parts of the network cell.

E. Atmospheric Parameters

Finally, let us collect all auxiliary formulas used to calculate necessary atmospheric parameters. To approximate the actual speed of wind (v_w) at the specific altitude h in the time step t , the following mathematical equation can be used [7]:

$$v_w(t, h) = v_w(t, h_{\text{WS}}) \cdot \frac{\ln((h + h_{\text{T}})/z_0)}{\ln(h_{\text{WS}}/z_0)}, \quad (13)$$

where h_{WS} , h_{T} , and z_0 are the absolute altitude, at which the measurement has been done (the altitude of the weather station – WS), terrain altitude, and surface roughness length, respectively. The air density (ρ) at the altitude h and in the current time step t can be calculated as follows [10]:

$$\rho(t, h) = \frac{p_d(t, h)}{R_d \cdot (T_a(t, h) + 273.15)} + \frac{p_v(t, h)}{R_v \cdot (T_a(t, h) + 273.15)}, \quad (14)$$

where R_d and R_v are the specific gas constants for dry air and water vapor, respectively. Next, p_d and p_v are the pressures of dry air and water vapor. The latter at the altitude h and in the time step t can be expressed by the formula [10]:

$$p_v(t, h) = 6.1078 \cdot 10^{\frac{7.5 \cdot T_a(t, h)}{T_a(t, h) + 237.3}}, \quad (15)$$

The pressure of dry air at the same altitude and moment has been described by $p_d(t, h) = p(t, h) - p_v(t, h)$, where p is the air pressure evaluated as [10]:

$$p(t, h) = p_0(t) \cdot e^{-\frac{g(h) \cdot M \cdot (h + h_{\text{T}} - h_0)}{R \cdot T_a(t, h)}}, \quad (16)$$

where p_0 is the air pressure at the reference level h_0 . It was assumed that the reference level is the sea level altitude ($h_0 = 0$). Next referring to [11], the gravitational acceleration is described by $g(h) = g_0 \frac{r_e^2}{(r_e + h)^2}$, where g_0 and r_e are the sea level acceleration and mean radius of the Earth, respectively. Finally, the formula to calculate the ambient temperature (T_a) at the altitude h and moment t is shown below [10]:

$$T_a(t, h) = T_a(t, h_{\text{WS}}) - 0.0065(h + h_{\text{T}} - h_{\text{WS}}). \quad (17)$$

V. SIMULATION SETUP

The source code of the developed software was prepared in Java language. The examination of the system scenario described in Section III has been performed in the form of 10 independent simulation runs each considering 4 days of the previous year starting different seasons – vernal equinox (20th March 2022), summer solstice (21st June 2022), autumn equinox (23rd September 2022), and winter solstice (21st December 2022). The parameters of users (location coordinates and traffic demand) have always been defined at the beginning of each simulation run. The assumed time step was equal to 1 hour ($4 \cdot 24 = 96$ steps per simulation run), with which the weather data was updated, and then the calculations for energy prosumption were carried out. The simulation setup for network and energy designs is highlighted in Tab. I and II.

TABLE I
NETWORK DESIGN CONFIGURATION [4], [5], [15], [16]

	Parameter	Sign	Unit	Value			
				Cell of Base Station			Mobile Station
				1 st	2 nd	3 rd	
Overall	Quantity	K	–	8			300
	Movement Speed	v	[m/s]	N/A			0
	Placement	–	–	N/A			outdoor
	Technology	–	–	5G			N/A
Band	Frequency	f	[MHz]	800	2100	3500	N/A
	Channel Bandwidth	B_w	[MHz]	80	120	120	N/A
	Used Subcarriers	$N_{\text{SC,u}}$	–	320			N/A
	Total Subcarriers	$N_{\text{SC,t}}$	–	512			N/A
	Sampling Factor	SF	–	1.536			N/A
	Pilot Reuse Factor	RF	–	1			N/A
	Coherence Time	t_c	[ms]	50			N/A
	Coherence Bandwidth	B_c	[MHz]	1			N/A
	TDD Duty Cycle DL	D_{DL}	[%]	75			N/A
	TDD Duty Cycle UL	D_{UL}	[%]	25			N/A
Transceivers	Spatial Duty Cycle	S	[%]	0	0	25	N/A
	Antenna Height	h	[m]	(32, 46)			1.5
	Antenna Elements	M	–	1	1	64	1
	Antenna Gain	G_a	[dBi]	16	18	24	0
	Antenna Feeder Loss	L_f	[dB]	2	2	3	0
	Max. Transmit Power	$P_{\text{TX,max}}$	[dBm]	46	49	53	23
	Noise Figure	NF	[dB]	8	8	7	N/A
	Path Loss Model	–	–	TR 38.901			N/A
	Interference Margin	IM	[dB]	2			0
	Doppler Margin	DM	[dB]	3			N/A
Propagation	Fade Margin	FM	[dB]	10			N/A
	Shadow Margin	SM	[dB]	12.8	15.2	10	N/A
	Implementation Loss	IL	[dB]	0	0	3	N/A
	Soft Handover Gain	G_{SHO}	[dB]	N/A			0

TABLE II
ENERGY PROSUMPTION CONFIGURATION [5], [6], [9]–[15], [18]–[20]

	Parameter	Sign	Unit	Value
Network Cell	Fixed Power Component	P_{FIX}	[W]	10
	Local Oscillator Power	P_{LO}	[W]	0.2
	Circuit Components Power	P_{CC}	[W]	0.4
	Encoding Power	P_{COD}	[W]	0.1
	Decoding Power	P_{DEC}	[W]	0.8
	Backhaul Traffic Power	P_{BT}	[W]	0.25
	Auxiliary Power	P_{AUX}	[W]	0
	Computational Efficiency	η_{BS}	[Gflops/W]	75
	Server Room (SR) Dimensions	$a_s \times b_s \times h_s$	[m]	7 x 5 x 3.5
	SR Target Temperature	T_s	[°C]	18
	SR Heat Transfer Coeff.	σ_s	-	2.037
	Circuit Heat Transfer Coeff.	σ_{CP}	-	0.9
	Cooling Loss Factor	σ_{cool}	-	0.1
	DC Loss Factor	σ_{DC}	-	0.075
	Amplifier Efficiency	μ_{PA}	-	0.35
PV Panels	Model	Solarland SLP020-12U		
	Nominal Voltage	$V_{n,PV}$	[V]	12
	Voltage at Max. Power	$V_{max,PV}$	[V]	17.2
	Current at Max. Power	$I_{max,PV}$	[A]	1.16
	Rated Power	$P_{R,PV}$	[W]	20
	Ground-relative Altitude	h_{PV}	[m]	(27, 41)
	Module Dimensions	$a_{PV} \times b_{PV}$	[m]	0.576 x 0.357
	Solar Radiation at STC	$G_{T,STC}$	[W/m ²]	1000
	Solar Radiation for NOCT	$G_{T,NOCT}$	[W/m ²]	800
	Temperature under STC	$T_{c,STC}$	[°C]	25
	Temperature NOCT	$T_{c,NOCT}$	[°C]	47
	Temperature Coeff. of Power	α_{PV}	[%/°C]	-0.5
	Solar Absorptance	α	-	0.3√10
	Solar Transmittance	τ	-	0.3√10
	Derating Factor	f_{PV}	-	0.723
	Number in Serial Order	$N_{PV,s}$	-	4
	Number in Parallel Order	$N_{PV,p}$	-	16
Total Number per Net. Cell	N_{PV}	-	64	
Wind Turbine	Model	Greatwatt S1000 1200W / 48V		
	Nominal Voltage	$V_{n,WT}$	[V]	48
	Rated Power	$P_{R,WT}$	[W]	1000
	Rated Wind Speed	v_r	[m/s]	10
	Cut-In Wind Speed	v_{in}	[m/s]	3
	Cut-Out Wind Speed	v_{out}	[m/s]	16.2
	Rotor Radius	r_{WT}	[m]	1.09
	Ground-relative Altitude	h_{WT}	[m]	(35, 49)
	Surface Roughness Length	z_0	[m]	3.0
	Air Density at STC	ρ_{STC}	[kg/m ³]	1.225
	Number of Rotor Blades	i_{WT}	-	3
	Number in Serial Order	$N_{WT,s}$	-	1
	Number in Parallel Order	$N_{WT,p}$	-	1
Total Number per Net. Cell	N_{WT}	-	1	
Battery System	Model	Solise Battery 48V 60Ah LiFePO ₄		
	Nominal Voltage	$V_{n,BATT}$	[V]	51.2
	Charging Voltage	$V_{c,BATT}$	[V]	57.6
	Discharging Voltage	$V_{d,BATT}$	[V]	51.2
	Charging Current	$I_{c,BATT}$	[A]	30
	Rapid Charging Current	$I_{r,BATT}$	[A]	50
	Discharging Current	$I_{d,BATT}$	[A]	50
	Capacity	C_{BATT}	[Ah]	60.78
	Provided Energy	$E'_{BATT,max}$	[Wh]	3112
	Max. Depth of Discharge	DoD _{max}	[%]	100
	Primary State of Charge	SoC _p	[%]	100
	Battery's Efficiency	μ_{BATT}	-	0.95
	Number of Cycles	N_{BC}	-	2000
	Number in Serial Order	$N_{BATT,s}$	-	1
Number in Parallel Order	$N_{BATT,p}$	-	6	
Total Number per Net. Cell	N_{BATT}	-	6	
Other	Reference Altitude	h_0	[m]	0
	Terrain Absolute Altitude	h_T	[m]	54.44
	Weather Station Absolute Alt.	h_{WS}	[m]	90
	Buildings Relative Altitude	h_{BU}	[m]	(27, 41)
	Mean Radius of the Earth	r_e	[m]	6371009
	Sea Level Gravitational Accel.	g_0	[m/s ²]	9.80665
	Air Molar Mass	m_{air}	[kg/mol]	0.0289644
	Universal Gas Constant	R_u	[$\frac{N \cdot m}{mol \cdot K}$]	8.31432
	Dry Air Gas Constant	R_d	[J / (kg · K)]	287.058
Water Vapor Gas Constant	R_v	[J / (kg · K)]	461.495	

VI. RESULTS

The results shown in Fig. 2 present achieved characteristics for battery system behavior according to the season of the year. The attached plots were prepared by averaging the state of charge of the battery systems of all cells over a specific

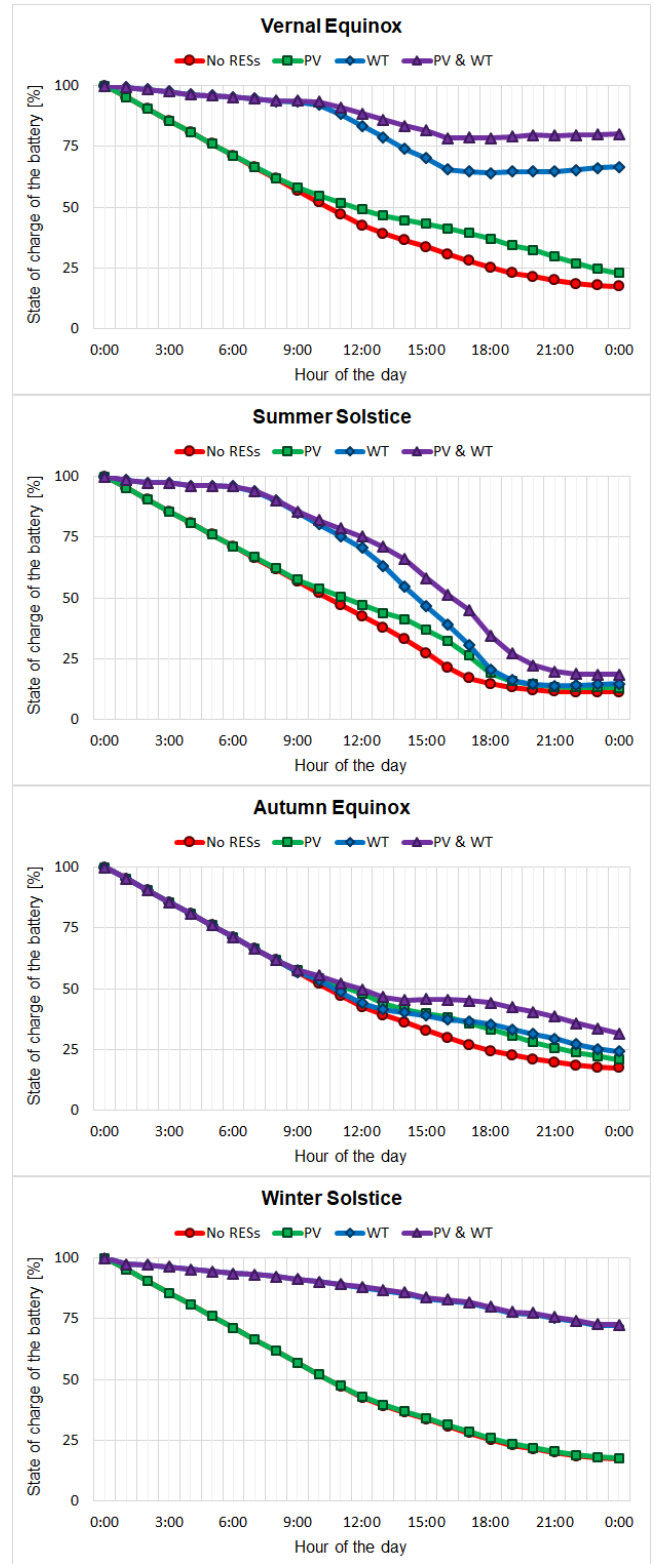


Fig. 2. Average state of charge of the battery in different seasons of the year.

time step from each simulation run. Based on the same data, the impact of using PV panels and wind turbines on extending the lifetime of a cell's battery system and reducing

energy consumption from conventional sources was included in Tab. III. By engaging RES generators within the wireless system, we were able to gain additional power support for the battery banks for each considered date. However, it can be noticed that much more effective type of RES generator (of the two presented) for the area specified by the weather conditions similar to the ones observed in Poland is the wind turbine. The most effective season from the perspective of using WTs is the winter solstice. On that day, the energy consumption from the electrical grid based on fossil fuels was reduced by about 74.24%. This in turn extended the lifetime of each battery on average by about 195.11% that day. As the second best case was the vernal equinox reducing the use of conventional resources and extending the battery lifetime by about 64.74% and 147.56%, respectively. Other dates were characterized by unfavorable wind conditions, i.e., too high (summer solstice) or too low (autumn equinox) speed of it for most of the day. Although the most solar energy resources were obtained during the summer solstice, the vernal equinox was much more efficient for equipping cells with PV panels (AEBL: 7.24%, AREC: 15.65%). The reason for that was the occurrence of additional power consumption caused by the need to cool the hardware in server rooms during high summer temperatures. For the rest of the dates, recorded solar radiation density values were at a very low level (especially for the winter solstice, where there are almost no energy savings). Furthermore, for the vernal equinox, the combination of both energy generator types was remarked to be the best solution in terms of the efficiency of supporting the existing grid of power lines (AEBL: 313.32%, AREC: 76.63%). Successively in the classification were the winter solstice (AEBL: 200.24%, AREC: 74.66%), autumn equinox (more efficient in AEBL than summer solstice), and summer solstice (more efficient in AREC than autumn equinox). From the perspective of the whole year, the most efficient solution was the deployment of both types of RES generators (AEBL: 70.24%, AREC: 50.69%).

VII. CONCLUSION

The contribution presented in this paper highlights the advantages related to the use of PV panels and wind turbines as power generators in 5G cellular networks. For the considered scenario, a very significant accomplishment has been observed. The power savings (and the resulting financial ones) exceeded the level of 50% per year in comparison to the case, in which the system is supplied only by the conventional energy grid. Although RESs are characterized by time-varying harvesting processes, by appropriate management of available resources (radio and energy) using optimizing algorithms (e.g., traffic steering, resource allocation, etc.) we are able to improve already achieved results or even ensure energy autonomy for cellular network without worsening the quality of mobile services delivered to users. However, the implementation of those algorithms will be taken into account in future work.

TABLE III
ENERGY CHARACTERISTICS FOR VARIOUS RES CONFIGURATIONS

	Total (and peak) energy obtained per cell [kWh]		
	PV Panels	Wind Turbine	PV & WT
Vernal Equinox	91.2 (0.48)	446.5 (1.27)	537.7 (1.56)
Summer Solstice	109.91 (0.73)	237.92 (1.21)	347.83 (1.39)
Autumn Equinox	67.09 (0.52)	107.54 (0.87)	174.63 (1.29)
Winter Solstice	3.39 (0.03)	460.91 (1.11)	464.31 (1.11)
Annual average	24, 783.63	114, 324	139, 107.6

	Average extension of battery lifetime (AEBL) [%]			
	No RESs	PV Panels	Wind Turbine	PV & WT
Vernal Equinox	0	7.24	147.56	313.32
Summer Solstice	0	1.96	3.94	8.62
Autumn Equinox	0	4.28	8.76	20.54
Winter Solstice	0	0.22	195.11	200.24
Annual average	0	3.34	51.15	70.24

	Average reduction in energy consumption (AREC) [%]			
	No RESs	PV Panels	Wind Turbine	PV & WT
Vernal Equinox	0	15.65	64.74	76.63
Summer Solstice	0	12.33	22.97	35.09
Autumn Equinox	0	10.93	17.33	27.52
Winter Solstice	0	0.64	74.24	74.66
Annual average	0	10.23	41.55	50.69

ACKNOWLEDGMENT

The cooperation between the authors has been initiated within the COST CA10210 INTERACT. M. Deruyck is a Post-Doctoral Fellow of the FWO-V (Research Foundation – Flanders, ref: 12Z5621N). The work by A. Samorzewski and A. Kliks was realized within project no. 2021/43/B/ST7/01365 funded by National Science Center in Poland.

REFERENCES

- [1] C. Freitag et al., „The climate impact of ICT: A review of estimates, trends and regulations”, arXiv: 2102.02622v1.
- [2] C. -L. I et al., „Energy-efficient 5G for a greener future”, *Nature Electronics*, vol. 3, pp. 182–184, 2020.
- [3] M. Deruyck et al., „Designing a multiple renewable energy source system to feed the wireless access network”, *Elsevier Sustainable Energy, Grids and Networks*, vol. 31, 2022.
- [4] G. Castellanos et al., „Multi-objective optimization of human exposure for various 5G network topologies in Switzerland”, *Computer Networks*, vol. 2016, 2022.
- [5] E. Björnson, J. Hoydis, and L. Sanguinetti, „Massive MIMO Networks: Spectral, Energy, and Hardware Efficiency”, *Foundations and Trends® in Signal Processing*, vol. 11, no. 3–4, pp. 154–655, 2017.
- [6] Y. Peng, Y. Shi, J. Li and Y. Hu, „Optimal Scheduling of 5G Base Station Energy Storage Considering Wind and Solar Complementation”, 2022 4th Asia Energy and Electrical Engineering Symposium (AEEES), Chengdu, China, 2022, pp. 384–389.
- [7] HOMER Pro v3.15, „Documentation – HOMER’s Calculations”, Available at: https://www.homerenergy.com/products/pro/docs/3.15/homers_calculations.html, Accessed: 25 April 2023.
- [8] C. Carrillo, A. F. Obando Montaña, J. Cidrás, and E. Díaz-Dorado, „Review of power curve modelling for wind turbines”, *Renewable and Sustainable Energy Reviews*, vol. 21, pp. 572–81, 2013.
- [9] Voltacon, „How long does it take to charge batteries from solar panels?”, Available at: <https://voltaconsolar.com/blog/2021/04/27/how-long-does-it-take-to-charge-batteries-from-solar-panels>, Accessed: 25 April 2023.
- [10] Omni Calculator, „Physics Calculators”, Available at: <https://www.omnicalculator.com/physics>, Accessed: 25 April 2023.
- [11] vCalc, „Gravity Acceleration by Altitude”, Available at: <https://www.vcalc.com/wiki/KurtHeckman/Gravity+Acceleration+by+Altitude>, Accessed: 25 April 2023.
- [12] Solarland, „Solarland SLP020-12U – Specifications”, Available at: <https://www.solar-electric.com/lib/wind-sun/SLP020-12U.pdf>, Accessed: 25 April 2023.

- [13] Greatwatt, „Greatwatt S1000 1200W / 48V – Specifications”, Available at: <https://energypower.gr/wp-content/uploads/2015/12/specifications10.pdf>, Accessed: 25 April 2023.
- [14] Solise, „Solise Battery 48V 60Ah LiFePO₄ – Specifications”, Available at: <https://solise.eu/gallery/Fiche%20technique%20batterie%2048V60.pdf>, Accessed: 25 April 2023.
- [15] System Informacji Przestrzennej (SIP), „Poznań – Model 3D”, Available at: <http://sip.poznan.pl/model3d/#/legend>, Accessed: 25 April 2023.
- [16] BTSearch, „Baza danych oraz mapa lokalizacji stacji BTS / pozwoleń UKE”, Available at: <http://beta.btsearch.pl>, Accessed: 25 April 2023.
- [17] Visual Crossing, „Historical Weather Data & Weather Forecast Data”, Available at: <https://www.visualcrossing.com/weather-data>, Accessed: 25 April 2023.
- [18] O. Arnold, F. Richter, G. P. Fettweis, and O. Blume, „Power Consumption Modeling of Different Base Station Types in Heterogeneous Cellular Networks”, IEEE, *Future Network & Mobile Summit*, 2010.
- [19] E. A. Franklin, „Calculations for a Grid-Connected Solar Energy System”, Available at: <https://extension.arizona.edu/sites/extension.arizona.edu/files/pubs/az1782-2019.pdf>, Accessed: 25 April 2023.
- [20] HOMER Pro v3.15, „Documentation – Glossary”, Available at: <https://www.homerenergy.com/products/pro/docs/3.15/glossary.html>, Accessed: 25 April 2023.